



**HAL**  
open science

# The diversity of radial variations of wood properties in European beech reveals the plastic nature of juvenile wood

Tancrede Alméras, Delphine Jullien, Shengquan Liu, Caroline Loup, Joseph Gril, Bernard Thibaut

## ► To cite this version:

Tancrede Alméras, Delphine Jullien, Shengquan Liu, Caroline Loup, Joseph Gril, et al.. The diversity of radial variations of wood properties in European beech reveals the plastic nature of juvenile wood. 2024. hal-04133248v6

**HAL Id: hal-04133248**

**<https://hal.science/hal-04133248v6>**

Preprint submitted on 6 Jan 2025

**HAL** is a multi-disciplinary open access archive for the deposit and dissemination of scientific research documents, whether they are published or not. The documents may come from teaching and research institutions in France or abroad, or from public or private research centers.

L'archive ouverte pluridisciplinaire **HAL**, est destinée au dépôt et à la diffusion de documents scientifiques de niveau recherche, publiés ou non, émanant des établissements d'enseignement et de recherche français ou étrangers, des laboratoires publics ou privés.

# The diversity of radial variations of wood properties in European beech (*Fagus sylvatica* L.) reveals the plastic nature of juvenile wood

ALMERAS Tancred<sup>1</sup>, JULLIEN Delphine<sup>1</sup>, LIU Shengquan<sup>2</sup>, LOUP Caroline<sup>3</sup>,  
GRIL Joseph<sup>4,5,\*</sup>, THIBAUT Bernard<sup>1</sup>

<sup>1</sup> LMGC, Univ Montpellier, CNRS, Montpellier, France

<sup>2</sup> School of Forestry & Landscape Architecture, Anhui Agricultural University, Hefei, China.

<sup>3</sup> Service du Patrimoine Historique, Univ Montpellier, Montpellier, France

<sup>4</sup> Université Clermont Auvergne, CNRS, Institut Pascal, Clermont-Ferrand, France

<sup>5</sup> Université Clermont Auvergne, INRAE, PIAF, Clermont-Ferrand, France

\* Corresponding author, email: [joseph.gril@cnrs.fr](mailto:joseph.gril@cnrs.fr)

## Keywords

Beech; Wood properties; Variability; Radial variation; Juvenile transition; Ontogenetic juvenility; Adaptive juvenility

## Abstract (395 words)

The long-term (as opposed to short-term intra-ring) radial variation of wood properties in European beech (*Fagus sylvatica* L.) from pith to bark are largest in the young ages of the tree (internal core). This so-called juvenility reflects both cambium ageing (ontogenetic juvenility) and adaptation to the changing mechanical constraints during secondary growth (adaptive juvenility). Ring width (*RW*), specific gravity (*SG*) and specific modulus (*SM*) are important parameters for each new wood layer, needed for the study of mechanical stability of a standing tree. They should be sensitive to the mechanical adaptation of growth. They were measured on diametrical boards (North/South direction) issued from 86 trees from several high forest stands in European countries. Analysis of variance showed very significant influence of position within the tree (core/external), of trees within a plot and of plots, but not for North/South orientation. The share of variance was similar for *SG* and *SM* (importance of tree effect) but different for *RW* (importance of plot effect). The occurrence of red heartwood in the core on some trees had a significant influence, mostly on *SM*, but the differences between white and red wood was very small. Globally the variability was high for *RW*, rather small for *SM* and very small for *SG*. Accordingly, the variations of the modulus of elasticity (product of *SG* and *SM*) were much more influenced by *SM* than by *SG* for beech. The radial variations of each parameter were fitted by both a linear (2 coefficients: zero value and mean slope) and a parabolic curve (3 coefficients: zero value, initial slope and curvature). They were used to classify types or radial profile in terms of flat, up & down and straight, convex & concave. Median values of coefficients per plot (or total) were used to draw median profiles for each parameter per plot and at the global level. The median global profiles differed from the typical radial pattern (TRP) of juvenility for plantation softwoods for *SG* (down concave instead of up concave) and *SM* (convex like TRP but with a clear decrease in the mature wood). The main result was the very large variability of profiles between trees or even between plots. Even if there is a part of ontogenetic influence in the juvenile patterns for *RW*, *SG* and *SM*, the results suggest that the influence of mechanical constraints on tree growth (adaptive juvenility) dominates largely.

45 **Notations and abbreviations**

46	<i>CV</i>	coefficient of variation
47	<i>D</i>	density
48	<i>L, L</i>	longitudinal direction, specimen length in L direction
49	<i>R, R</i>	radial direction, specimen length in R direction
50	<i>RW</i>	ring width
51	<i>SG</i>	specific gravity (ratio of <i>D</i> over water density)
52	<i>SM</i>	specific modulus (squared value of sound speed in L direction)
53	<i>T, T</i>	tangential direction, specimen length in T direction
54	TRP	typical radial pattern
55	<i>W</i>	specimen weight

56 **1. Introduction**

57 Wood is a material that results from competition for height growth in the terrestrial  
 58 environment, which is submitted to tremendous physical constraints such as gravity, wind and  
 59 drought. The functions of wood (mechanical support, conduction and storage) respond these  
 60 constraints, and are fulfilled by different cell types (fibres or tracheids, vessels and  
 61 parenchyma). In tree species, the bulk of wood material is generally made of fibres, which have  
 62 mainly a mechanical function. Despite their major importance for tree functioning and survival,  
 63 other cell types generally represent only a small part of wood in terms of biomass investment.  
 64 Actually, most of terrestrial biomass is in the form of fibres (Bar-on et al 2017). This massive  
 65 investment in fibres points to the major significance of the mechanical constraint for trees. The  
 66 viewpoint that we will adopt here is that the amount and quality of wood products are mainly  
 67 responses to the mechanical requirement of the tree to face the two major constraints that are  
 68 wind and gravity.

69 Trees are built through wood growth (Thibaut 2019) including simultaneously primary growth  
 70 by elongation or creation of twigs and secondary growth by thickening of existing axes.  
 71 Secondary growth is performed by living wood cells in the cambial zone: stem cells of cambium  
 72 itself and daughter cells (Raven et al 2007, Savidge 2003, Déjardin et al 2010, Thibaut 2019).  
 73 It consists of the following successive steps: division of the cambium stem cells into daughter  
 74 cells; expansion of daughter cells until the end of primary wall formation; thickening of fibre  
 75 cell walls until the end of secondary wall formation; lignification of the whole cell wall,  
 76 including the compound middle lamella; programmed fibre and vessel cell death.

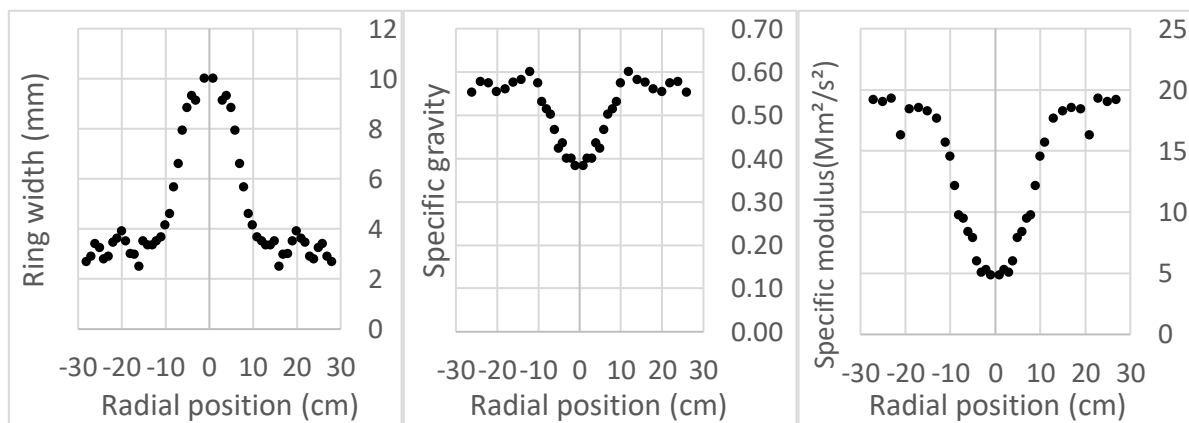
77 The cambial activity results in tree rings (in temperate tree species) and local wood properties  
 78 that often differ from ring to ring. They can be described by ring width (*RW*), result of combined  
 79 cell division and expansion, specific gravity (*SG*) resulting from the ratio between cell wall  
 80 thickening and expansion, and specific modulus (*SM*) mainly determined by the organisation  
 81 of the secondary cell wall (micro-fibril angle of the S2 layer) (Cave 1969). These three features  
 82 determine most parameters involved in the adaptation to mechanical constraints. For a trunk of  
 83 a given height, the rigidity against lateral wind forces depends on trunk diameter (related to  
 84 *RW*) and on wood modulus of elasticity (MOE) which is the product of *SG* and *SM* (Fournier  
 85 et al. 2013). For a given biomass investment, there is a trade-off between *RW* (large growth  
 86 rate) and *SG* (large density). The flexibility of the trunk depends inversely on diameter, and  
 87 positively on wood deformability (equal to the ratio of strength to modulus of elasticity, which  
 88 is negatively correlated to *SM* as can be seen on wood database, e.g. Ross 2010). The  
 89 mechanical stability of the tree depends on its diameter, modulus of elasticity (product of *SG*  
 90 by *SM*), and inversely on its green density (correlated to *SG*, Dlouha et al 2018). The postural  
 91 control (Alméras & Fournier 2009) depends on the asymmetry in radial growth rate (related to  
 92 *RW*), modulus of elasticity, and maturation strain (often correlated to *SM*, Alméras et al 2005).

93 Mechanical adaptation is therefore a matter of fine-tuning of wood properties, accounting for  
 94 the trade-offs between them.

95 The secondary growth descriptors (*RW*, *SG*, *SM*) display spatial variation within a segment of  
 96 the trunk, in the 3 cylindrical directions: transversely across radii (Tar), around the perimeter  
 97 (Ap) and longitudinally along the stem (Las), called variation “TarApLas” within the tree by  
 98 Savidge (2003). The variations around the perimeter in a given ring are related to posture  
 99 control (Alm eras and Fournier 2009), either due to trunk inclination (Alm eras et al 2005, Dassot  
 100 et al. 2015) or to orientation change of the branches after apex death (Loup et al 1991). The  
 101 variations along the stem are related to primary growth: i) succession of connected zones and  
 102 free-from-branching portions of the axis and ii) ageing of the terminal bud along the successive  
 103 growth units. Apart in the vicinity of the branching zones, these variations are rather slow  
 104 (Savidge 2003).

105 Radial variations from pith to bark at a given height can be divided in two types: i) intra-ring  
 106 short distance changes mostly due to seasonal effects and ii) variations of mean ring properties,  
 107 reflecting adaptations to changes in mechanical constraints during ontogeny. These mechanical  
 108 constraints change according to the size of the tree (Fournier et al. 2013). The largest variations  
 109 in dimensions and environment occur during the young ages. As a result, radial variations of  
 110 these properties display larger gradients in the centre of a stem than in its periphery. This defines  
 111 the “juvenile wood” or the “core wood”, depending on the authors (Lachenbruch et al 2011).

112 The steep radial variations in juvenile wood were nicely described by Bendtsen & Senft (1986).  
 113 Loblolly pine (*Pinus taeda* L.) (Fig. 1 and Fig. 2) shows a typical radial pattern (TRP) of  
 114 juvenility (Lachenbruch et al 2011): initial increase of tracheid length, specific gravity (*SG*) and  
 115 specific modulus (*SM*), initial decrease of ring width (*RW*). The initial segment with steep  
 116 changes in properties corresponds to juvenile wood, and is followed by rings with more stable  
 117 properties called mature wood (which nevertheless may reveal interannual variations related to  
 118 climate and mechanical constraints). Such patterns are generally observed in in conifer  
 119 plantations (softwood trees). This is the general case in softwood plantation trees (Cown &  
 120 Dowling 2015, Larson et al 2001).



121  
 122 Fig. 1. Juvenility for mechanical indicators in Loblolly pine, after Bendtsen & Senft (1986): from pith  
 123 to bark, according to the typical radial pattern, ring width decreases, specific gravity increases and  
 124 specific modulus decreases.

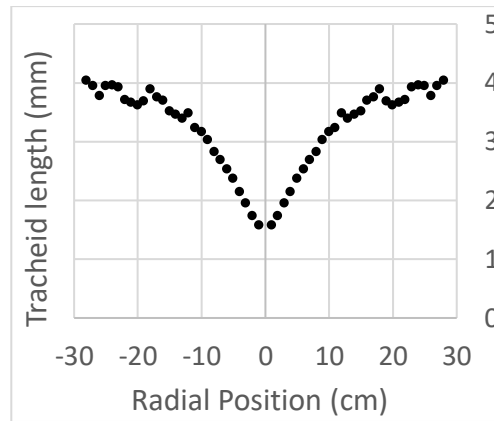


Fig. 2. Juvenility for tracheid length in Loblolly pine, after Bendtsen & Senft (1986):  
typical increase from pith to bark.

125  
126  
127

128 Variations in tracheid or fibre length always share the same initial positive gradient for all trees  
129 (Fig. 2), whether softwood or hardwood (Koubaa et al 1998, Larson et al 2001, Bhat et al 2001,  
130 Bao et al 2001, Kojima et al 2009). This parameter is important for paper industry (Koubaa et  
131 al 1998) but is not cited as a factor influencing wood mechanical properties (Kollmann & Côté  
132 1968, Kretschman 2010).

133 The variation of parameters characterizing wood structure and properties depends on tree  
134 ontogeny and adaptation to changing constraints during its life. *Juvenility* describes the  
135 evolution of wood parameters during the early years of the stem. An important question is to  
136 separate the genetically programmed changes in properties with ontogeny (here termed  
137 *ontogenetic juvenility*) from the plastic adaptation to changing constraints (here termed *adaptive*  
138 *juvenility*). The systematic nature of juvenile gradients in fibre length suggest that they are  
139 consequence of cambium ageing (ontogenetic juvenility). Here we aim at investigating whether  
140 juvenile variations in three functional wood properties (*RW*, *SG* and *SM*) depend on plastic  
141 adaptation or on prescribed ontogenetic changes. It will be considered, for a given property,  
142 that ontogenetic changes are characterised by similar patterns of radial variations among a large  
143 sampling, while plastic adaptation corresponds to a large variability of radial patterns between  
144 trees and between populations.

145 For that a sampling covering a wide diversity of geographical locations and forest management  
146 practices was needed. The data obtained on a large panel of beech trees will be exploited to  
147 characterize the patterns of radial variations of wood mechanical indicators in beech.  
148 Hypotheses that will be discussed are the following: i) most of the variation are similar all  
149 around the trunk (profile symmetry); ii) all the trees share the same radial pattern (ontogenetic  
150 juvenility) within the different growing conditions.

151 In healthy beech trees, heartwood and sapwood can scarcely be distinguished. A so-called “red  
152 heartwood”, which is a kind of chemical discoloration, is often observed (Liu et al 2005) and it  
153 affects the commercial value of the wood (Trenčiansky et al 2017). The hypothesis that red  
154 wood occurrence does not affect mechanical parameters will also be tested.

## 155 2. Material and methods

### 156 2.1. Material

157 Nine plots representative of forest management of beech (*Fagus sylvatica* L.) in Western  
158 Europe (Becker & Beimgraben 2001, Jullien et al 2013) were selected (Table 1). Up to ten trees  
159 per plot (86 in total) were selected for the measurement of wood properties (Table 1). All trees  
160 were dominant or co-dominant and their mean diameter at breast height was around 60 cm  
161 (Table 2).

162

Table 1. Characteristics of the studied plots

	age (years)	Plot								
		1	2	3	4	5	6	7	8	9
Forest:	Nb trees	10	10	10	10	10	8	10	10	8
Even-aged	100-130	o		o	o	o	o			
Even-aged (mountain)	120-150		o						o	
Uneven-aged	60-120							o		
Middle to even-aged forest	60									o
Height	m	32.6	32.1	35.5	36.1	36	38.3	34	39.2	35.3
Slenderness	mm/m	58.3	65	58.9	64	64.9	61.7	60.2	68	47.6
DBH	cm	56	49.4	60.7	56.6	55.4	62.5	56.9	58.2	74.5

163

Table 2. Geometric description of the 86 selected trees

86 trees	Mean	Min	Max	CV
Height (m)	35.4	23.7	42.6	10.1%
Slenderness (mm/m)	61.3	41.0	80.4	13.2%
Diameter (cm)	58.5	47.0	84.5	13.2%

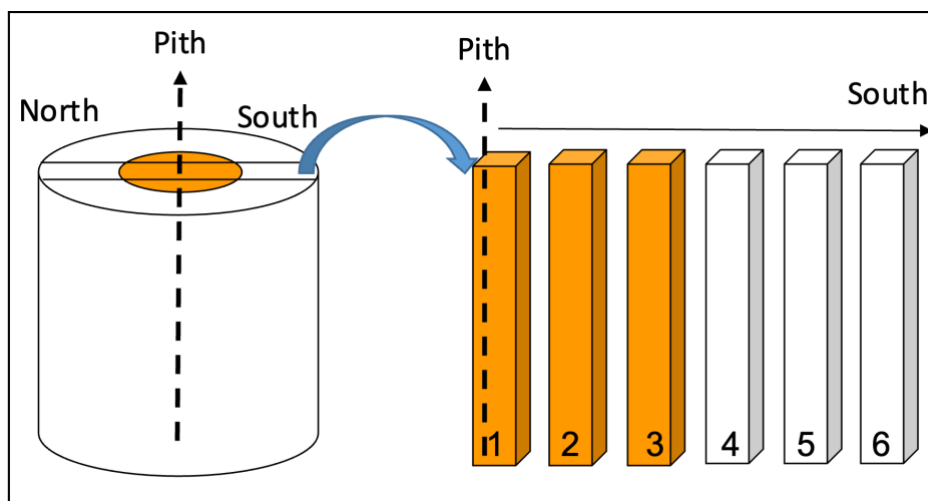
Min: minimum value; max: maximum value; CV: coefficient of variation

164

165

166 One small log of 50 cm length was cut at a height of 4 m for each tree. Each small log was cut  
 167 into radial boards, through the pith, from North to South (North direction was carved in the log  
 168 bark). These boards were air-dried to an average moisture content of 13.5 % and cut into 1259  
 169 rods of 20 mm in radial, 20 mm in tangential and 360 mm in longitudinal direction, from the  
 170 pith outwards (Fig. 3). The rods with irregularities or cracks were discarded.

171 The rods were numbered according to their position in the board, their distance to pith was  
 172 measured, and their orientation (North or South) was noted. At the same time, the number of  
 173 rings at both ends of the samples was recorded and the mean annual ring width of the rod (*RW*)  
 174 was calculated as the ratio of the mean radial dimension to the number of rings. Each sample  
 175 located at a distance lower than 10 cm from the pith was considered as a “core” sample. The  
 176 presence of red heartwood was also noted for the rods located in the core (Liu et al 2005).



177

178 Fig. 3. Diagram of the sawing of the rod after the sawing of a North-South diametrical board.  
 179 Numbering both for Northern and Southern parts of the board start with pith position. The coloured  
 180 parts evoke the case of red heartwood occurrence.

181 **2.2. Measurement of properties.**

182 Density ( $D$ ) was calculated by measuring the weight ( $W$ ) and the dimensions  $R$ ,  $T$ ,  $L$  of the rod:  
 183  $D = W/(R.T.L)$ . The specific gravity ( $SG$ ) was the ratio between  $D$  and water density.

184 To measure the specific modulus ( $SM$ ,  $10^6\text{m}^2/\text{s}^2$ ), each rod was positioned on fine wires and set  
 185 in free vibration by a hammer stroke. The analysis of the sound vibration by fast Fourier  
 186 transform gave the values of the three highest resonance frequencies, which were interpreted  
 187 using equations yielding an estimate of  $SM$  where the contribution of longitudinal shear to the  
 188 bending deformation has been eliminated (Brancheriau & Baillères 2002).

189 **2.3. Statistical analyses**

190 The measured wood properties ( $RW$ ,  $SG$ ,  $SM$ ) playing a role in stem construction and being  
 191 linked to the 3 successive phases of living wood cells in the cambial zone (cell division, cell  
 192 expansion and cell-wall thickening), and each phase being influenced by the mechanical and  
 193 hydraulic constraints on the tree during wood growth, it is expected that their variations are  
 194 related to each other. Therefore, distribution of properties and correlations between them will  
 195 have to be computed at various level (between rods, between trees and between plots).

196 2.3.1 Correlations and basic statistics

197 Basic statistical analyses were performed using XLSTAT software. The normality of the  
 198 distribution was verified by Shapiro-Wilk test. A Pearson correlation analysis was used in the  
 199 case of a normal distribution, and a Spearman correlation analysis in the case of a non-normal  
 200 distribution, which was the majority of cases.

201 2.3.2 Analysis of variance and variance components

202 Analyses of variance (ANOVA) and variance components analyses (VCA) were carried out  
 203 using R software (R Core Team 2018). A first set of analyses tested the effect of the different  
 204 factors on the three measured variables, using a nested ANOVA design where a random “tree”  
 205 factor was nested within the “plot” factor, and the “core” factor nested within the “tree” factor.  
 206 Sample orientation (North or South) was accounted for through an independent “orientation”  
 207 factor.

208 Another set of ANOVA and VCA was carried out to test the effect of red heartwood on wood  
 209 properties. This analysis was based only on core specimens, as red heartwood occurs only on  
 210 these specimens. As both the measured properties and the occurrence of red heartwood were  
 211 correlated to the distance to the pith (red heartwood occurs more often in inner parts of the  
 212 core), its effect was tested with a two-ways ANOVA, with specimen number and red heartwood  
 213 occurrence (Red) as two independent factors. A VCA was carried out on this model to quantify  
 214 the share of variance of each factor.

215 2.3.3 Quantitative analysis of radial profiles

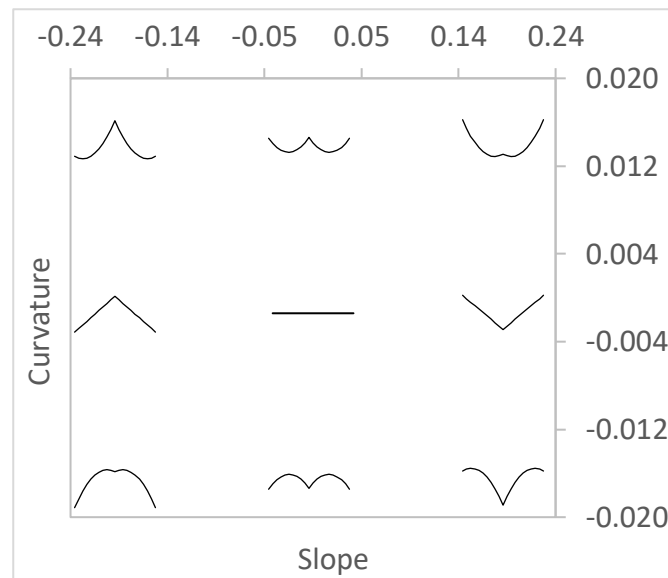
216 North and South radial profiles were analysed together, yielding 172 profiles on which the rod-  
 217 averaged value of the three variables ( $RW$ ,  $SG$  and  $SM$ ) have been quantified as a function of  
 218 the distance to the pith. We built a Microsoft Excel file to view and analyse these profiles (see  
 219 Suppl. Mat.). The purpose of this analysis was the quantification of the shapes of these profiles,  
 220 and how they correlate between properties or vary between plots. To achieve this, we  
 221 considered two main indicators of each profile’s shape: the slope, and the curvature.

222 The slope of the particular radial profile was computed as the coefficient of the linear regression  
 223 between the considered property and the distance to the pith. It indicates whether the property  
 224 is globally increasing, decreasing, or staying constant. The curvature was computed as the  
 225 coefficient of quadratic term of a second-degree polynomial regression. A positive value  
 226 corresponds to a convex shape, where the local slope increases outward, whereas a negative

227 value corresponds to a concave shape, where the slope decreases outward. All combinations of  
 228 slope and curvature can exist. Thus, each profile could be represented as a dot on a  
 229 slope/curvature graph, corresponding to a particular shape. The correspondence between  
 230 parameter's values and profile shapes is illustrated on Fig. 4, where the 'icons' illustrate the  
 231 symmetric shape corresponding to their position on the graph.

232 The correlations between quantitative parameters of the profiles were studied through a PCA  
 233 (carried out using R) taking into account the following 15 variables for each of the 172 radial  
 234 profiles: the mean value of the property ( $RW_m$ ,  $SG_m$ ,  $SM_m$ ), the global slope ( $RW_s$ ,  $SG_s$ ,  
 235  $SM_s$ ) obtained from the linear regression, the initial value of the property ( $RW_{a0}$ ,  $SG_{a0}$ ,  
 236  $SM_{a0}$ ), the initial slope of the property ( $RW_{a1}$ ,  $SG_{a1}$ ,  $SM_{a1}$ ) and the curvature ( $RW_{a2}$ ,  
 237  $SG_{a2}$ ,  $SM_{a2}$ ), obtained as the coefficients of the second-degree polynomial regression.

238 At the plot level, we computed the median and the interquartile range of each parameter (slope  
 239 and curvature) on each variable ( $RW$ ,  $SG$  and  $SM$ ), to appreciate whether there were systematic  
 240 differences in profile shapes between plots. An ANOVA was used to test the effect of the plot  
 241 factor on each parameter.



242  
 243 Fig. 4. Illustration of the correspondence between profile parameters (slope and curvature) and shape  
 244 of a symmetric profile ("flying bird" icons).  
 245

246 The 172 profiles were then classified according to two criteria: they were classified as "Flat",  
 247 "Up" or "Down" according to a threshold on the slope, and as "Straight", "Convex" or  
 248 "Concave" according to a threshold on the curvature. We used a criterion based on the  
 249 magnitude of the effect of each parameter rather than on its statistical significance. Indeed, in  
 250 many cases the significance of the slope (or curvature) was found high (low P-value) although  
 251 the magnitude of the effect was weak when compared to the overall range of variation of the  
 252 parameter. The threshold values were set at an arbitrary 50% of the overall standard deviation  
 253 of each variable, scaled by the mean distance to the pith (10 cm) for the slope, and by its square  
 254 for the curvature. At the tree level, the diametral profiles (including both North and South  
 255 profiles) were classified as symmetric ("Sym") if parameters of the North and South profiles  
 256 differed less than a threshold defined consistently with above (see suppl. mat.).



257 **3. Results**258 **3.1. Effect of red heartwood on wood properties**

259 The effect of red heartwood on wood properties was tested on core specimens only, accounting  
 260 for the distance to the pith (specimen number) as an independent factor. The results (Table 3)  
 261 show that the distance to the pith was always a significant factor while red heartwood was non-  
 262 significant for *RW* and *SG*.

263 Table 3. Results of the variance component analysis of the effect of red heartwood occurrence (Red)  
 264 and specimen number (Num, indicating the distance to the pith) on the properties of core specimens:  
 265 share of variance for each factor (%) and significance of the factors

Factor	<i>RW</i>	<i>SG</i>	<i>SM</i>
Num	2.5**	2.7***	3.0***
Red	ns	ns	8.6***

266 \*\*\*  $P < 10^{-3}$ ; \*\*  $P < 10^{-2}$ ; ns  $P > 0.05$ ; *RW*: ring width; *SG*: specific gravity; *SM*: specific modulus

267 Contrary to our expectations, the effect of red heartwood on the specific modulus was found  
 268 significant, representing a substantial share of variance (8.6%). Its occurrence is associated to  
 269 a lower *SM* ( $-0.67 \cdot 10^6 \text{ m}^2/\text{s}^2$  in average, 3% of the mean value), even when the effect of distance  
 270 to the pith was accounted for. Pöhler et al (2006) found significant difference ( $p < 0.05$ ) both for  
 271 density and modulus of elasticity. But the two parameters were higher for red heartwood (+3%  
 272 and +6% respectively, which means +3% for *SM*). One reason for the difference could be due  
 273 to a modification of cell wall properties during the expansion of red heartwood. Another one  
 274 could be that trees with lower *SM* were more prone to develop red heartwood in our sampling.  
 275 Anyway, in both studies, the difference between red heartwood and white heart density and  
 276 specific modulus was quite small. Therefore, it will not be considered in the following analysis.

277 **3.2 Structuration of variance at the within-tree, between-tree and between-plot levels**

278 ANOVA was highly statistically significant for each of the three measured variables (*RW*, *SG*  
 279 and *SM*). Plot, tree within plot and core within tree were all very highly significant factors ( $P <$   
 280  $10^{-6}$ ) for the three variables, while orientation was a significant factor only for *SM* ( $P =$   
 281 0.00012). The share of variance of each factor for each variable is displayed in Table 4, together  
 282 with the statistical significance of each factor. For *RW*, the core factor (inner 10 cm radius,  
 283 compared to the outer zone) represented the largest part of variance, followed by the plot and  
 284 tree factors. For *SG* and *SM*, the tree factor was the largest part of variance. The orientation  
 285 factor was statistically significant only for *SM* with a very low share of variance and a very low  
 286 difference in mean value for North (637 rods; mean value =  $22.1 \cdot 10^6 \text{ m}^2/\text{s}^2$ ) and South (622  
 287 rods; mean value =  $22.4 \cdot 10^6 \text{ m}^2/\text{s}^2$ ).

288 Table 4. Results of the variance component analysis of the effect of Plot, Tree, Core and Orientation  
 289 factors on the properties of all specimens: share of variance for each factor (%) and significance  
 290 of the factors

Factor	<i>RW</i>	<i>SG</i>	<i>SM</i>
Plot	21.9***	14.0***	15.4***
Plot/tree	9.2***	36.4***	28.6***
Plot/tree/core	29.5***	18.2***	14.6***
Orientation	ns	ns	0.8***
Error	39.4	31.4	40.6
Total	100	100	100
Total Within-Tree	68.9	49.6	56.0

291 \*\*\*  $P < 10^{-3}$ ; ns  $P > 0.05$ ; *RW*: ring width; *SG*: specific gravity; *SM*: specific modulus

292 **3.3. Correlations between properties at different levels**

293 **3.3.1. Rod level**

294 Table 5 shows descriptors of the distribution of properties for all samples (1259 rods). The  
295 variation of *SG* between samples was very low (coefficient of variation 6.2%) compared to that  
296 of *SM* (10.9%) and *RW* (35%).

297

298 *SG* and *SM* were correlated positively (Table 6). *RW* was correlated positively with *SG* and  
299 negatively with *SM*. These correlations were very significant (below the 0.1% level) although  
300 they were quantitatively rather weak, explaining only 5% to 10% of variance.

301

302

Table 5. Parameter description for all rods

1259 rods	<i>RW</i>	<i>SG</i>	<i>SM</i>
Minimum	0.67	0.55	11.08
Maximum	6.67	0.83	27.49
Mean	2.30	0.69	22.22
Max/min	10.00	1.51	2.48
C.V.	35.0%	6.2%	10.9%

303

*RW*: ring width (mm); *SG*: specific gravity; *SM*: specific modulus ( $10^6\text{m}^2/\text{s}^2$ )

304

Table 6. Spearman correlation table between the three measured parameters, at rod level

1259 rods	<i>RW</i>	<i>SG</i>	<i>SM</i>
<i>RW</i>	1	0.16***	-0.33***
<i>SG</i>	0.16***	1	0.12***
<i>SM</i>	-0.33***	0.12***	1

305

\*\*\*  $P < 10^{-3}$ ; ns:  $P > 0.05$ ; *RW*: ring width; *SG*: specific gravity; *SM*: specific modulus

306 **3.3.2. Tree level**

307 Table 7 shows the descriptors of the distribution of mean values of properties per tree.  
308 Variability at the tree level, as quantified by the coefficients of variation, was significantly  
309 lower than for the rod level, and notably low for *SG*. This result was consistent with the fact  
310 that a substantial part of the variance was at the within-tree level (Table 4, “Core” factor).

311

Table 7. Parameter description for tree mean values

86 trees	<i>RW</i>	<i>SG</i>	<i>SM</i>
Minimum	1.29	0.63	17.6
Maximum	4.78	0.78	25.6
Mean	2.28	0.70	22.4
Max/min	3.70	1.24	1.46
C.V.	24.9%	4.8%	7.6%

312

*RW*: ring width (mm); *SG*: specific gravity; *SM*: specific modulus ( $10^6\text{m}^2/\text{s}^2$ )

313

314 At the between-tree level, only the negative correlation between *RW* and *SM* remained  
315 significant (Table 8), showing that trees with higher growth rates (higher mean *RW*) had lower  
316 *SM*. Note that the correlation between these properties was even higher in magnitude at the tree  
317 level (-0.40) than at the rod level (-0.33).

318 Table 8. Spearman correlation table between the three measured parameters, at tree level

86 trees	<i>RW</i>	<i>SG</i>	<i>SM</i>
<i>RW</i>	<b>1</b>	0.08 <sup>ns</sup>	-0.40 <sup>***</sup>
<i>SG</i>	0.08 <sup>ns</sup>	<b>1</b>	0.16 <sup>ns</sup>
<i>SM</i>	-0.40 <sup>***</sup>	0.16 <sup>ns</sup>	<b>1</b>

319 \*\*\* P<10<sup>-3</sup>; ns: P>0.05; *RW*: ring width; *SG*: specific gravity; *SM*: specific modulus

### 320 3.3.3. Plot level

321 Table 9 shows the descriptors of the distribution of mean values of properties per plot.  
322 Variability at the plot level, as quantified by the coefficients of variation, was significantly  
323 lower than for the tree level, consistent with the large part of variance at the between-tree level  
324 (Table 4, “Tree” factor).

325 Table 9 Parameter description for the 9 plots mean values

Plot	<i>RW</i>	<i>SG</i>	<i>SM</i>
1	2.06	0.70	21.5
2	1.80	0.71	23.1
3	2.63	0.70	22.2
4	2.50	0.71	21.2
5	2.12	0.68	21.9
6	2.57	0.73	23.7
7	2.84	0.68	22.0
8	1.63	0.68	24.1
9	2.50	0.67	21.7
Maximum	2.84	0.73	24.1
Minimum	1.63	0.67	21.2
Mean	2.29	0.70	22.4
C.V.	16.9%	2.6%	4.2%

326 *RW*: ring width (mm); *SG*: specific gravity; *SM*: specific modulus (10<sup>6</sup>m<sup>2</sup>/s<sup>2</sup>)

327

328 At the plot level no correlation was detectable between parameters (Table 10).

329 Table 10. Spearman correlation table between the three measured parameters, at plot level

9 Plots	<i>RW</i>	<i>SG</i>	<i>SM</i>
<i>RW</i>	<b>1</b>	0.18 <sup>ns</sup>	-0.17 <sup>ns</sup>
<i>SG</i>	0.18 <sup>ns</sup>	<b>1</b>	0.23 <sup>ns</sup>
<i>SM</i>	-0.17 <sup>ns</sup>	0.23 <sup>ns</sup>	<b>1</b>

330 ns: P>0.05; *RW*: ring width; *SG*: specific gravity; *SM*: specific modulus

331

## 332 3.4. Diversity of radial profiles of properties

### 333 3.4.1 Illustration of profile diversity

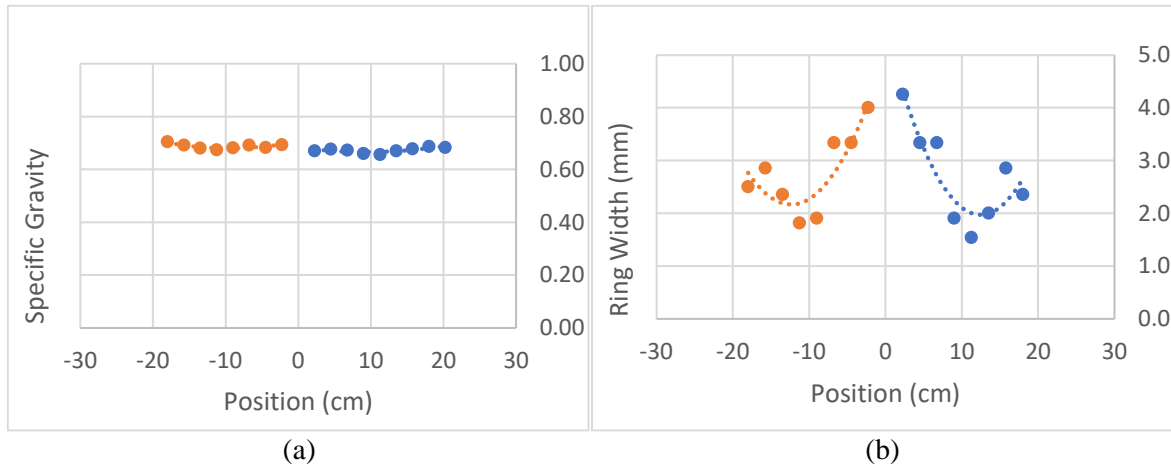
334 A total of 516 profiles (86 trees x 2 orientations x 3 variables) were observed and analysed. The  
335 mean coefficients of determination (R<sup>2</sup>) of the regressions was 0.43 for linear regression, and  
336 0.61 for second-degree polynomial regressions, showing that the quadratic term captured a  
337 large part of profile non-linearity.

338 Examples of typical profiles together with the second-degree fitting are shown in Fig. 5 (all  
339 profiles can be viewed from the file provided as supplementary material). The chosen examples

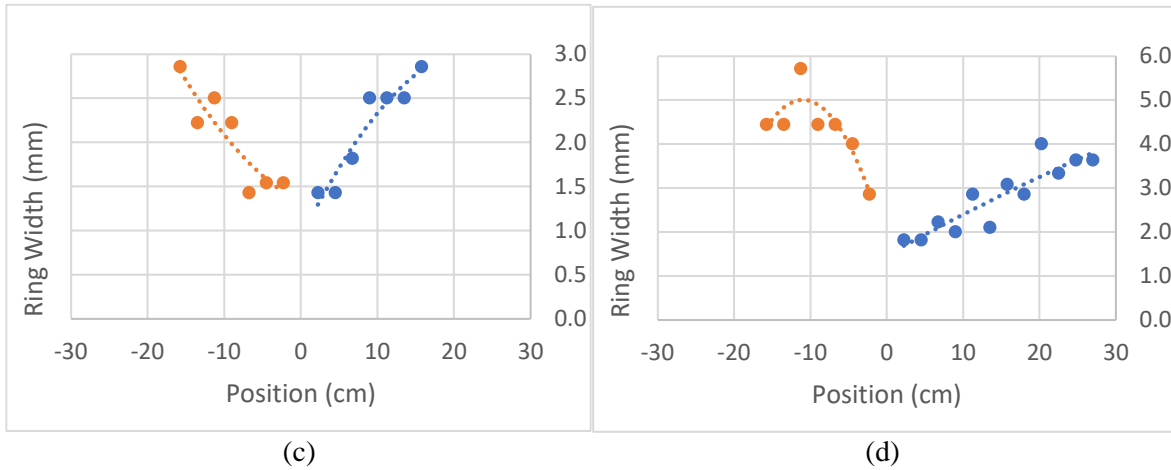
Radial variations of beech properties

340 illustrate the diversity of the diametral profiles, with symmetric profiles (a, b, c, e) as well as  
 341 non-symmetric profiles (d, f). The radial profiles were either flat (a), increasing (c, d, e-South,  
 342 f) or decreasing (b), and either straight (a, c, d-North), convex (b, f-North) or concave (d-South,  
 343 e, f-South).

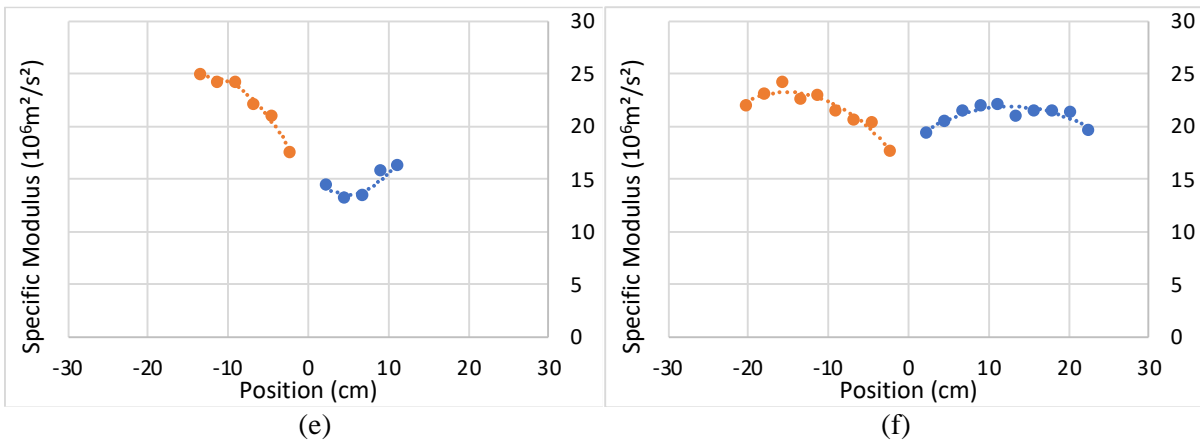
344  
 345



346  
 347



348  
 349



350  $10^6$  Fig. 5. Examples of property profiles: (a) tree 694, plot 6; (b) tree 443, plot 4;  
 351 (c) tree 290, plot 2; (d) tree 1050, plot 9; (e) tree 1025, plot 9; (f) tree 299, plot 2

352

353 3.4.2 Typology of profiles

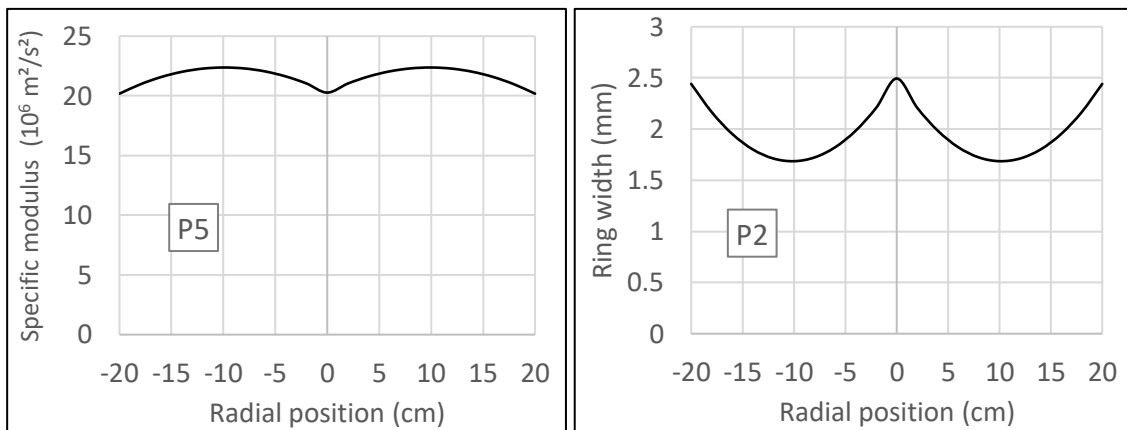
354 For each of the three studied variables there was a large diversity of radial profiles, with  
 355 instances of all nine possible combinations of slope (“Up”, “Flat”, “Down”) and curvature  
 356 (“Convex”, “Straight”, “Concave”). Nevertheless, the frequency of these different shapes  
 357 differed (Table 11). The proportion of symmetric profiles (“Sym”) is about one third, showing  
 358 that most trees display substantial variations of properties around the periphery.

359 Table 11. Occurrence of profile types, characterised by the pattern of radial variation from pith to  
 360 bark, for 172 North and South cases

N + S	Sym	Flat	Up	Down	Straight	Convex	Concave
<i>RW</i>	36%	41%	18%	41%	36%	37%	27%
<i>SG</i>	37%	42%	13%	45%	48%	34%	19%
<i>SM</i>	28%	42%	37%	20%	28%	10%	62%

361 *RW*: ring width; *SG*: specific gravity; *SM*: specific modulus

362 The proportion of flat radial profiles was of about 40% for each variable. Most other profiles  
 363 were decreasing for *RW* and *SG*, and increasing for *SM*. But less than 50% of flat profiles were  
 364 straight, meaning that most flat profiles were either convex (for *RW* or *SG*), or concave (as for  
 365 *SM*) (Fig. 6).  
 366

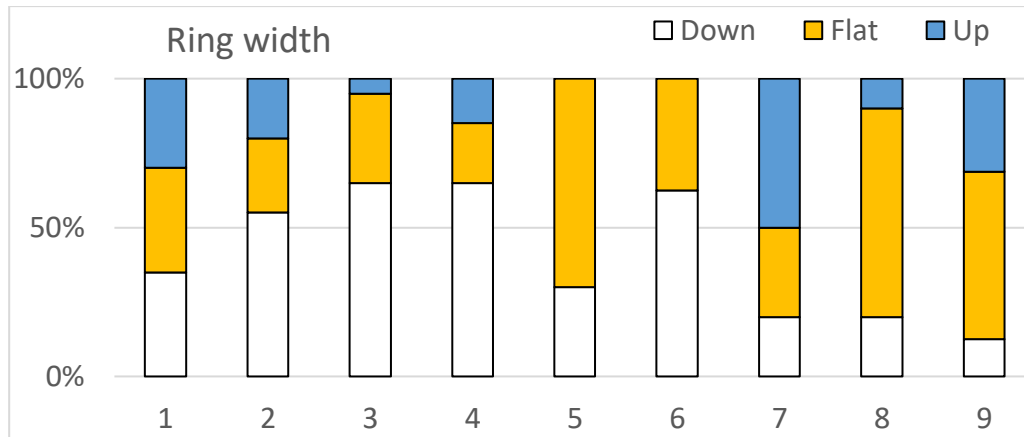


367 Fig. 6. Examples of median plot profiles with flat slope:  
 368 flat-convex (Specific modulus, plot 5) or flat-concave (Ring width, plot 2)  
 369  
 370

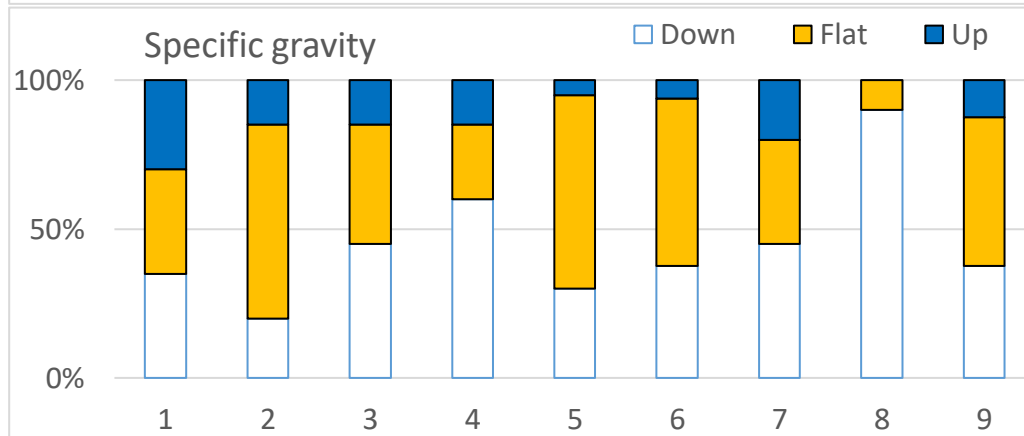
371 The proportions of each type of profile seemed to differ between plots, as illustrated on Fig. 7.

## Radial variations of beech properties

372



373



374

375

376

377

Fig. 7. Distribution of profile types for the 9 plots, based on the slope of the linear regression of the studied properties versus the radial position

378

### 3.4.3 Distribution of profiles shape parameters

379

380

381

382

The median shape of all radial profiles is illustrated on Fig. 8. These profiles were “down-convex” for *RW* and *SG*, and “up-concave” for *SM*. The shape of the median profile of each plot can be viewed from the supplementary material.

## Radial variations of beech properties

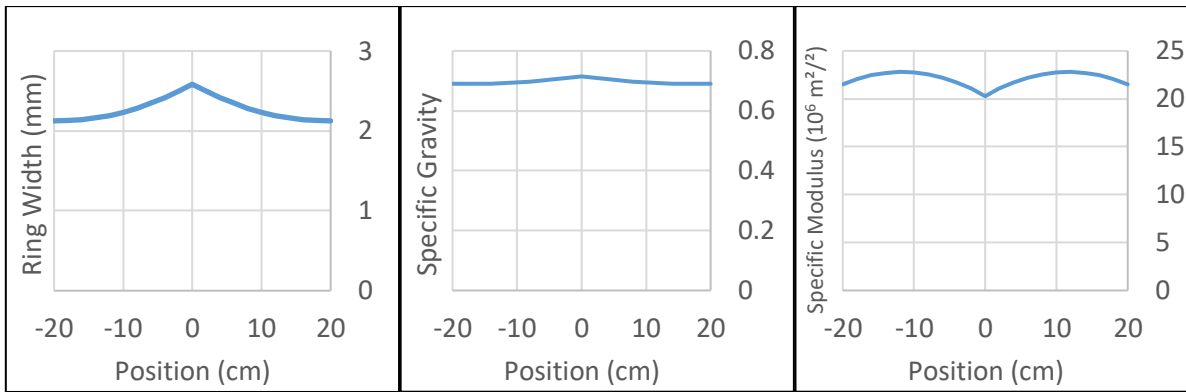


Fig.8 Median profiles over all trees, mixing both orientations in a symmetrical presentation.

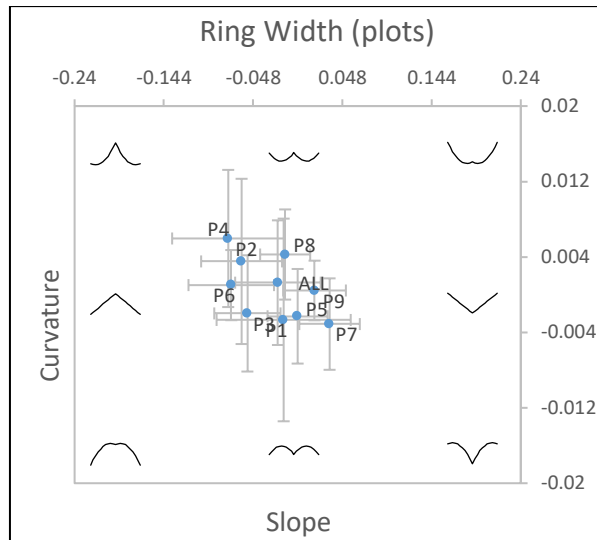
383  
384  
385

386 The distribution of profile shape parameters is illustrated in Fig. 9. Each figure represents the  
387 distribution (median and inter-quartile) of parameters (slope and curvature) for each plot,  
388 together with “icons” illustrating the correspondence between the position on the graph and the  
389 profile shape. The figures are centred on zero on the X and Y axis, so that the centre of the  
390 figure represents the flat straight profile, and each quadrant of the figure represents a type of  
391 profile. A similar figure representing the distribution of parameter from individual radial  
392 profiles is provided in supplementary material.

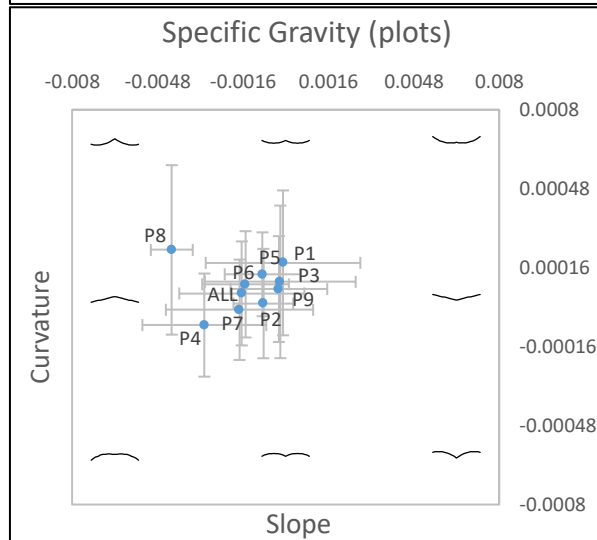
393 It is apparent from Fig. 9 that shape parameters of profiles were not randomly distributed. The  
394 plot effect on the slope parameter was found significant for all three variables, while its effect  
395 on curvature was found significant only for *SG*.

Radial variations of beech properties

396



397



398

399

400

401

402

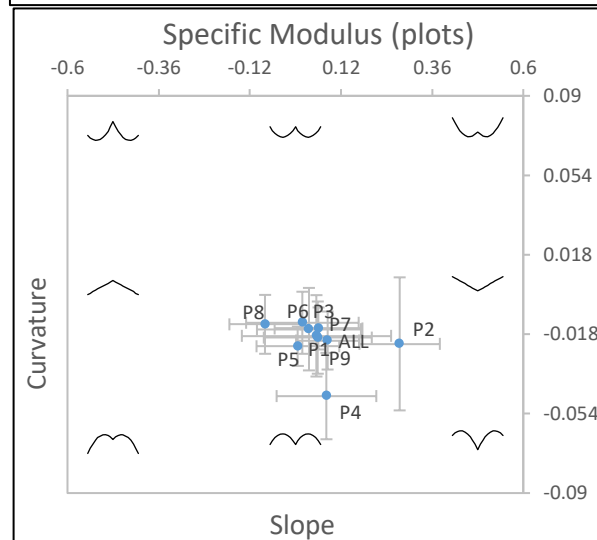


Fig. 9. Distribution of median plot profiles in the slope/curvature plane. Error bars represent the interquartile range of each plot. “Flying-bird” icons represent the shape associated to their position in the figure (see Fig. 4).

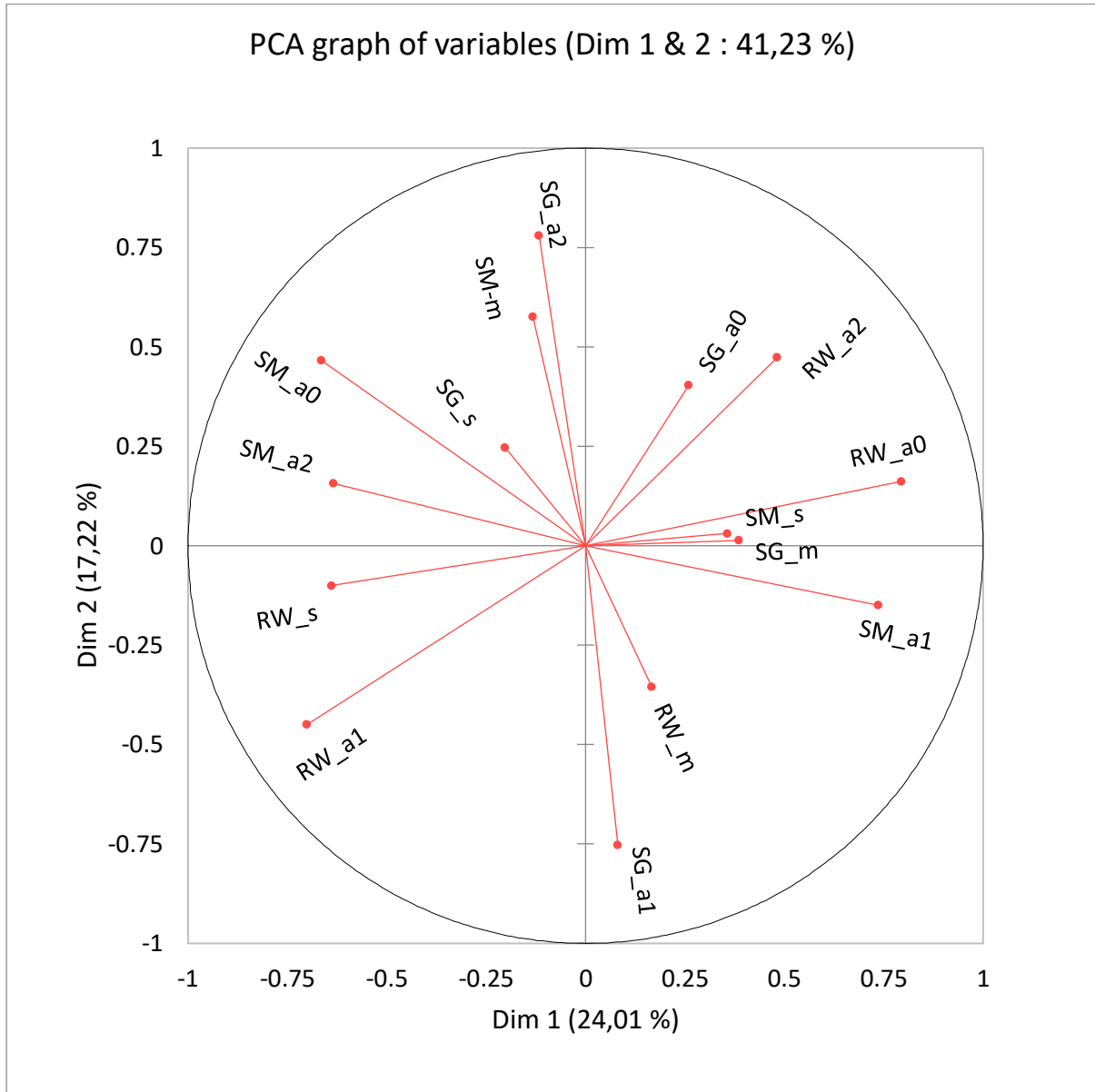


403 3.4.4 Correlations between profile shape parameters

404 The correlations between shape parameters of the profiles are illustrated in Fig. 10. The first  
 405 axis of this PCA opposed high initial ring width ( $RW_{a0}$ ) and positive initial slope of specific  
 406 modulus ( $SM_{a1}$ ) to high initial specific modulus ( $SM_{a0}$ ) and positive slope of ring width  
 407 ( $RW_{a1}$ ). This axis opposed high growth rate to high cell wall stiffness.

408 It is apparent that the initial slope ( $_{a1}$ ) and curvature ( $_{a2}$ ) were negatively correlated for all  
 409 three variables. It suggests that the quickest the variable was initially changing, the more this  
 410 rate of change was lowered during growth.

411



412

413 Fig. 10. Principal Component Analysis of shape profile parameters.

414  $RW$ : ring width;  $SG$ : specific gravity;  $SM$ : specific modulus

415  $_{-m}$ : mean value of the property;  $_{-s}$ : global slope obtained from the linear regression,

416  $_{-a0}$ ,  $_{-a1}$ ,  $_{-a2}$ : initial value, initial slope and curvature, respectively, obtained as the

417 coefficients of the second-degree polynomial regression.

418

## 419 **4. Discussion**

### 420 ***4.1. Interpretation of correlations between properties***

421 As a result of the large difference of variability between *SG* and *SM* (Table 5) the variability of  
 422 the modulus of elasticity which is the product of *SG* and *SM*, is more dependent on the variations  
 423 of *SM* than on the variations of *SG* in beech: The  $R^2$  of the linear regression between MOE and  
 424 *SG* is only 0.26, while that of the regression between *SG* and *SM* is 0.78.

425 Correlations between *RW* and both *SG* and *SM* were very highly significant, with a positive  
 426 value for *SG* (density is higher for large ring width) and a negative one for *SM* (specific modulus  
 427 is lower for large rings). These results were partly due to covariations along the juvenility  
 428 gradient that will be analysed in the next paragraph.

429 There was no significant correlation between *SG* and *SM*. This can be interpreted as a global  
 430 independence in mechanical adaptation of the two parameters: *SG* reflects the quantity of cell  
 431 wall (cell wall relative thickness), and *SM* its quality (microfibril angle), and these two  
 432 parameters can be regulated independently.

### 433 ***4.2. Major importance of within-tree variations in properties***

434 The importance of within-tree variations can be deduced from Table 4. Within-tree variation is  
 435 the share of variance that is not captured by higher scale factors (“Plot” and “Tree”), so it is the  
 436 sum of the “Core” factor, the “Orientation” factor and the “Error” factor (Table 4). Within-tree  
 437 variations represented approximately 65% of variance for *RW*, 50% for *SG* and 55% for *SM*.

438 The within-tree variations of properties originated from both peripheral variations and radial  
 439 variations. Peripheral variations were reflected by the frequent occurrence of non-symmetric  
 440 diametral profiles: for all 3 studied variables, most trees presented important differences  
 441 between North and South profiles (Table 11, Fig. 5). Radial variations were reflected by the  
 442 importance of the “Core” effect (Table 4), and by the non-zero values of slope and curvature  
 443 parameters of most radial profiles (section 3.3.3).

### 444 ***4.3. The frequency of non-symmetric diametral profiles reveals the importance of the gravity*** 445 ***constraint and posture control mechanisms.***

446 Most diametral profiles were asymmetric (Table 11) despite the fact that the “Orientation”  
 447 factor had no systematic effect on wood properties (Table 4). This is because the tree  
 448 asymmetry, if any, due to stem inclination (linked to the effect of wind or soil instability),  
 449 asymmetric crown (linked to the adaptation to light availability), and/or prevailing winds, had  
 450 only few reasons to be North/South. It is thus not surprising to find insignificant systematic  
 451 effect of orientation in the sampling.

452 The tree asymmetry induces mechanical constraints in relation to how trees manage gravity.  
 453 The growth of an asymmetric tree induces a rapid increase of the bending moment applied by  
 454 gravity of the trunk, which tends to bend the tree downwards. To counteract this effect, a  
 455 gravitropic reaction is needed (Alméras & Fournier 2009, Gril et al 2017). This reaction is  
 456 achieved by a dissymmetry of growth forces on the two sides of the inclined stem: a higher  
 457 tensile force on the upper side for hardwood species like beech. The tensile force produced on  
 458 each side of the tree during wood maturation process is proportional to ring width, to specific  
 459 gravity, to specific modulus and to maturation strain (Alméras et al 2005, Thibaut et Gril 2021).  
 460 Increasing the force on the upper side means increasing the local value of any combination of  
 461 these four factors, together with decreasing it on the lower side. This leads to asymmetric  
 462 profiles of wood properties.

463 Reaction wood occurrence is the typical expression of strong gravitropic reactions, influencing  
 464 the asymmetry in *RW*, *SG*, *SM*, and the asymmetry in maturation strains, that results from

465 macromolecular processes occurring during secondary wall formation (Alm eras and Clair 2016,  
 466 Thibaut and Gril 2021). However, for small inclination angles (e.g. coppice stems) the  
 467 production of tension wood is not necessary: the difference in maturation strain between normal  
 468 wood located on lower and upper sides of the growing stem can be high enough to enable  
 469 posture control (Thibaut and Gril 2021). Tension wood occurrence is rather easy to detect by  
 470 visual observation but variations of maturation strain in normal wood are, until now, impossible  
 471 to estimate except by *in-situ* measurements of residual stress at stem periphery (Jullien et al  
 472 2013).

#### 473 **4.4. Diversity in radial profiles suggests that “adaptive juvenility” is prevailing over** 474 **“ontogenetic juvenility”**

475 Most of the papers on mechanical properties of juvenile wood refer to plantation, either of  
 476 softwoods or hardwoods (Bensend and Senft 1986, Kojima et al 2009, Bhat et al 2001, Bao et  
 477 al 2001). For softwoods, the “typical radial pattern” for mechanical factors (Lachenbruch et al  
 478 2011) is always the case for fast-growing plantations. It is characterized by a decrease of *RW*  
 479 and an increase of both *SG* and *SM* from pith to bark until a juvenile core limit.

480 For hardwoods this is not always the case, and *SG* can be more or less flat (Bendtsen & Senft  
 481 1986), while *SM* can be high near the pith and decrease for trees growing in dense tropical forest  
 482 (Mc Lean et al 2011). On *Bagassa guianensis* Aubl, a fast-growing secondary forest tree of  
 483 French Guiana, Bossu et al (2018) observed a typical radial pattern for microfibril angle and  
 484 density, very clear for density (varying from 0.3 to 0.9 along the radius). Plourde et al (2015)  
 485 studied radial density variation for 91 tropical species (Costa Rica): 42 over 74 had a net  
 486 variation in density, 37 with increasing TRP type and 5 with decreasing “anti TRP” type.  
 487 Secondary forest species (open environment in juvenile phase) had the clearest positive  
 488 variations (low juvenile density), primary forest species (closed environment in juvenile phase)  
 489 were the only anti-TRP species, with a lower variation (high internal density). Beech in this  
 490 study is rather similar to trees from the primary forest with an internal density above 0.5 and a  
 491 decreasing profile. Longuetaud et al (2017) studied 3 broadleaved trees: oak, beech, sycamore  
 492 maple and two softwoods: fir and Douglas fir. The TRP model was valid for maple and Douglas  
 493 fir, but for oak the density decreased instead of increasing. For fir and beech, the profile was  
 494 bell-shaped (beech) or U-shaped (fir) with slight variations. Purba et al (2021) studied density  
 495 and microfibril angle in oak and beech for dominated, small-diameter trees harvested during  
 496 thinning. Overall, the TRP applied to both cases.

497 For beech, we have measured parameters describing the juvenility of old trees in managed forest  
 498 with a rather large variety of plot environment and management practices. The median profiles  
 499 for each mechanical parameter (beech radial pattern in Fig. 8) was similar to some hardwood  
 500 description in literature for *SG*.

501 In Europe, old growth beech forests can have different silviculture regimes Ciancio et al 2006):  
 502 even-aged (France or Germany) or uneven-aged high forest (Switzerland), coppicing with  
 503 standards (France) or conversion of coppice forest into high forest (Germany, France) but are  
 504 very rarely the result of plantations (none in the 9 plots). *Fagus* is known for its shade tolerance  
 505 and ability to grow very slowly under a closed canopy (Collet et al 2011) and most forest plots  
 506 undergo more or less severe thinning before final harvesting, which leads to an increase of *RW*  
 507 due to better access to light (Noyer et al 2017). This is reflected in the different mean *RW* radial  
 508 patterns for the 9 plots (Fig. 9). For plots 7 (uneven-aged high forest) and 9 (middle forest  
 509 transformed in even-aged high forest), a clear increase of *RW* was observed in the young ages,  
 510 while the reverse and classical pattern was true for plots 1, 4, 5 and 6 (all even-aged forest in  
 511 flat area). Similar results were found on younger beech trees (Bouriaud et al 2004). The low  
 512 *RW* values for plots 2 and 8 (even aged, steep terrain) could be expected in a mountainous area,  
 513 and the observed increase of *RW* after an initial decrease possibly due to thinning operations.

514 Probably due to the large diversity of plot management, the beech median radial pattern did not  
 515 apply to many trees of the sampling. As a result, there was no “universal” juvenile trend for any  
 516 of the 3 parameters for all trees. Combining global trend (flat, up, down) and curvature (straight,  
 517 convex, concave), there was a large variety of profile occurrence in each of the 9 cross-types  
 518 for each plot.

519 If the variation of properties had been governed by ontogenetic determinism, similar trends  
 520 would have been expected among trees and plots. The observed variability of radial variations  
 521 suggests, on the contrary, a dominance of plastic adaptation to mechanical constraints in the tree  
 522 growth (adaptive juvenility).

## 523 **5. Conclusion**

524 Based on the analysis of variance and the analysis of radial profiles, we showed that, for the 3  
 525 studied variables (*RW*, *SG* and *SM*) within-tree variations represented the largest part of  
 526 variance. These within-tree variations occurred both through peripheral variations (asymmetry  
 527 between North and South profiles) and through radial variations (dependence of the property  
 528 on the distance to the pith). The patterns of radial variations of the 3 variables were diverse,  
 529 including increasing, flat and decreasing patterns, as well as convex, straight and concave  
 530 patterns. Overall, these observations demonstrate that juvenile wood in Beech did not obey to  
 531 systematic variations (ontogenetic juvenility), but was the result of plastic adaptation (adaptive  
 532 juvenility) to variable individual trajectories and associated mechanical constraints.

533 One hypothesis that should be tested is the influence of change in access to light between trees  
 534 of the same species in similar environment, with very different initial growing condition: i)  
 535 understorey beginning like in primary forest, ii) plantation at very high density, iii) plantation  
 536 at low density, using heliophilic, semi-tolerant and shade-tolerant species (Lehnebach et al  
 537 2019). Measurement of radial variations of fibre length, ring width, basic specific gravity and  
 538 specific modulus should be made with narrow spacing (each 2 mm) near the pith and larger  
 539 ones (10 mm) nearer to the bark, in order to see if the transition between radial trend from one  
 540 mode to the other is close to pith or not. Another study should be done on plantation trees with  
 541 well documented forest management: initial spacing (high and low), date and importance of  
 542 thinning.

543 Moreover, basic studies should be made on modelling growing trees with large difference in  
 544 slenderness evolution and radial evolution of specific gravity and specific modulus as found in  
 545 this study. Radial evolution of maturation strain can be added with different hypotheses for  
 546 better representation of trunk growth. The tree stability (buckling or flexure risk) at each  
 547 growing step will be documented.

## 548 **Acknowledgments**

549 The data were obtained thanks to the support of European Commission through the FAIR-  
 550 project CT 98-3606, coordinated by Prof. Gero Becker. The financial support of CNRS K. C.  
 551 Wong post-doctoral program and China Scholarship Council must be also acknowledged.

## 552 **Supplementary material**

553 A Microsoft Excel file macros named “Data\_Hetre+Profils\_Final.xlsx” is available at the  
 554 following url:

555 <https://zenodo.org/records/14606666>

556 It contains the raw and elaborated data used in this paper, visualisation of property profiles and  
 557 results of analysis.

558 **References**

- 559 Alméras T, Thibaut A, Gril J. 2005. Effect of circumferential heterogeneity of wood maturation  
560 strain, modulus of elasticity and radial growth on the regulation of stem orientation in trees.  
561 *Trees* 19 (4), 457-467. <https://doi.org/10.1007/s00468-005-0407-6>
- 562 Alméras T., Fournier M. 2009. Biomechanical design and long-term stability of trees:  
563 Morphological and wood traits involved in the balance between weight increase and the  
564 gravitropic reaction. *Journal of Theoretical Biology* 256: 370–381.  
565 <https://doi.org/10.1016/j.jtbi.2008.10.011>
- 566 Alméras T, Clair B. 2016. Critical review on the mechanisms of maturation stress generation  
567 in trees. *Journal of the Royal Society, Interface* 13(122), 20160550.  
568 <https://doi.org/10.1098/rsif.2016.0550>
- 569 Bao FC, Jiang ZH, Jiang XM, Lu XX, Luo XQ, Zhang SY. 2001. Differences in wood  
570 properties between juvenile wood and mature wood in 10 species grown in China. *Wood  
571 Science and Technology* 35:363-375. <https://doi.org/10.1007/s002260100099>
- 572 Bar-On YM, Phillips R, Milo R. 2018. The biomass distribution on Earth. *Proceedings of the  
573 National Academy of Sciences*, 115(25), 6506-6511. <https://doi.org/10.1073/pnas.1711842115>
- 574 Bhat KM, Priya PB, Rugmini P. 2001. Characterisation of juvenile wood in teak. *Wood Science  
575 and Technology* 34:517-532. <https://doi.org/10.1007/s002260000067>
- 576 Becker G, Beimgraben T. 2001. Occurrence and relevance of growth stresses in Beech (*Fagus  
577 sylvatica* L.) in Central Europe. Final Report of FAIR-project CT 98-3606, Coordinator Prof.  
578 G. Becker, Institut für Forstbenutzung und forstliche Arbeitwissenschaft, Albert-Ludwigs  
579 Universität, Freiburg, Germany.
- 580 Bendtsen BA, Senft J. 1986. Mechanical and anatomical properties in individual growth rings  
581 of plantation-grown eastern cottonwood and Loblolly pine. *Wood and Fiber Science* 18(1): 23-  
582 38.
- 583 Bossu J, Lehnebach R, Corn S, Regazzi A, Beauchene J, Clair B. 2018. Interlocked grain and  
584 density patterns in *Bagassa guianensis*: changes with ontogeny and mechanical consequences  
585 for trees. *Trees - Structure and Function*, 32(6):1643-1655. [https://doi.org/10.1007/s00468-  
586 018-1740-x](https://doi.org/10.1007/s00468-018-1740-x).
- 587 Bouriaud O, Bréda N, Le Moguédec G, Nepveu G. 2004. Modelling variability of wood specific  
588 gravity in beech as affected by ring age, radial growth and climate. *Trees* 18:264–276.  
589 <https://doi.org/10.1007/s00468-003-0303-x>
- 590 Brancheriau L, Baillères H. 2002. Natural vibration analysis of wooden beams: a theoretical  
591 review. *Wood Science and Technology*, 36(4):347-365. [https://doi.org/10.1007/s00226-002-  
592 0143-7](https://doi.org/10.1007/s00226-002-0143-7)
- 593 Cave ID. 1969. The Longitudinal Young's Modulus of *Pinus Radiata* *Wood Science and  
594 Technology*, Vol. 3, p. 40-48
- 595 Ciancio O, Corona P, Lamonaca A, Portoghesi L, Travaglini D. 2006. Conversion of clearcut  
596 beech coppices into high forests with continuous cover: A case study in central Italy. *Forest  
597 Ecology and Management* 224: 235–240. <https://doi.org/10.1016/j.foreco.2005.12.045>
- 598 Collet C, Fournier M, Ningre F, Hounzandji AP, Constant T. 2011. Growth and posture control  
599 strategies in *Fagus sylvatica* and *Acer pseudoplatanus* saplings in response to canopy  
600 disturbance. *Annals of Botany* 107, 1345–1353. <https://doi.org/10.1093/aob/mcr058>
- 601 Cown D, Dowling L. 2015. Juvenile wood and its implications. *NZ Journal of Forestry*,  
602 February 2015, Vol. 59, No. 4: 10-17

- 603 Dassot M, Constant T, Ningre F, Fournier M. 2015. Impact of stand density on tree morphology  
604 and growth stresses in young beech (*Fagus sylvatica* L.) stands. *Trees*, [https://doi.org/10.1007/s00468-](https://doi.org/10.1007/s00468-014-1137-4)  
605 [014-1137-4](https://doi.org/10.1007/s00468-014-1137-4)
- 606 Déjardin A, Laurans F, Arnaud D, Breton C, Pilate G, Leplé JC. 2010. Wood formation in  
607 Angiosperms. *C. R. Biologies* 333 (2010) 325–334.
- 608 Dlouhá J, Alméras T, Beauchêne J, Clair B, Fournier M. 2018. Biophysical dependences among  
609 functional wood traits. *Functional Ecology*, 32(12), 2652-2665. [https://doi.org/10.1111/1365-](https://doi.org/10.1111/1365-2435.13209)  
610 [2435.13209](https://doi.org/10.1111/1365-2435.13209)
- 611 Fournier M, Dlouha J, Jaouen G, Alméras T. 2013. Integrative biomechanics for tree ecology:  
612 beyond wood density and strength. *Journal of Experimental Botany*, 64(15), 4793-4815.  
613 <https://doi.org/10.1093/jxb/ert279>
- 614 Gril J, Jullien D, Bardet S, Yamamoto H. 2017. Tree growth stress and related problems.  
615 *Journal of Wood Science*, 63 (5), 411-432. <https://doi.org/10.1007/s10086-017-1639-y>
- 616 Jullien D, Widmann R, Loup C, Thibaut B. 2013. Relationship between tree morphology and  
617 growth stress in mature European beech stands. *Annals of forest science* 70 (2), 133-142.  
618 <https://doi.org/10.1007/s13595-012-0247-7>
- 619 Kojima M, Yamamoto H, Yoshida M, Ojio Y, Okumura K. 2009. Maturation property of fast-  
620 growing hardwood plantation species: A view of fiber length. *Forest Ecology and Management*  
621 257: 15–22. <https://doi.org/10.1016/j.foreco.2008.08.012>
- 622 Kollmann FFP, Côté AA. 1968. Principles of wood Science and Technology, I. Solid Wood,  
623 Springer-Verlag, New York. <https://link.springer.com/book/10.1007/978-3-642-87928-9>
- 624 Koubaa A, Hernandez RE, Baudouin M, Poliquin J. 1998. Inter clonal, intra clonal and within-  
625 tree variation of fiber length of poplar hybrid clones. *Wood and Fiber Science* 30(1): 40-47
- 626 Kretschmann DE. 2010. Mechanical properties of wood. In *Wood handbook: Wood as an*  
627 *engineering material*. General Technical Report FPL-GTR-190. Madison: Forest Products  
628 Laboratory, USDA, Forest Service.
- 629 Lachenbruch B, Moore J, Evans R. 2011. Radial variation in wood structure and function in  
630 woody plants, and hypotheses for its occurrence. In: Meinzer FC, Lachenbruch B, Dawson TE  
631 (eds) *Size- and age-related changes in tree structure and function*. Springer, Dordrecht: 121–  
632 164.
- 633 Larson PR, Kretschmann DE, Clark AIII, Isebrands JG. 2001. Formation and properties of  
634 juvenile wood in southern pines: a synopsis. Gen. Tech. Rep. FPL-GTR-129. Madison, WI:  
635 U.S. Department of Agriculture, Forest Service, Forest Products Laboratory. 42 p.
- 636 Lehnebach R, Bossu J, Va S, Moel H, Amusant N, Nicolini E, Beauchêne J. 2019. Wood density  
637 variations of legume trees in french guiana along the shade tolerance continuum: hardwood  
638 effects on radial patterns and gradients. *Forests* 10, 80. <https://doi.org/10.3390/f10020080>
- 639 Longuetaud F, Mothe F, Santenoise P, Diop N, Dlouha J, Fournier M, Deleuze C. 2017. Patterns  
640 of within-stem variations in wood specific gravity and water content for five temperate tree  
641 species. *Annals of Forest Science* 74:64. <https://doi.org/10.1007/s13595-017-0657-7>
- 642 Loup C, Fournier M, Chanson B. 1991. Relations entre architecture mécanique et anatomie de  
643 l'arbre : cas d'un Pin Paritime (*Pinus pinaster* Soland.). *L'arbre, biologie et développement*.  
644 *Naturalia monspeliensa* N° hors série (C. Edelin ed)
- 645 Liu S, Loup C, Gril J, Dumonceaud O, Thibaut A, Thibaut B. 2005. Studies on European beech  
646 (*Fagus sylvatica* L.): variations of colour parameters. *Annals of Forest Science*, 62: 625-632.  
647 <https://doi.org/10.1051/forest:2005063>

- 648 Mc Lean JP, Zhang T, Bardet S, Beauchêne J, Thibaut A, Clair B, Thibaut B. 2011. The  
649 decreasing radial wood stiffness pattern of some tropical trees growing in the primary forest is  
650 reversed and increases when they are grown in a plantation. *Annals of Forest Science* 68: 681-  
651 688. <https://doi.org/10.1007/s13595-011-0085-z>
- 652 Noyer E, Lachenbruch B, Dlouhá J, Collet C, Ruelle J, Ningre F, Fournier M. 2017. Xylem  
653 traits in European beech (*Fagus sylvatica* L.) display a large plasticity in response to canopy  
654 release. *Annals of Forest Science* 74: 46, <https://doi.org/10.1007/s13595-017-0634-1>
- 655 Plourde BT, Boukili VK, Chazdon RL. 2015. Radial changes in wood specific gravity of  
656 tropical trees: inter- and intraspecific variation during secondary succession. *Functional*  
657 *Ecology*, 29:111–120. <https://doi.org/10.1111/1365-2435.12305>
- 658 Pöhler E, Klingner R, Künniger T. 2006. Beech (*Fagus sylvatica* L.) – Technological properties,  
659 adhesion behaviour and colour stability with and without coatings of the red heartwood. *Ann.*  
660 *For. Sci.* 63 (2006) 129-137. <https://doi.org/10.1051/forest:2005105>
- 661 Purba CYC, Dlouha J, Ruelle J, Fournier M. 2021. Mechanical properties of secondary quality  
662 beech (*Fagus sylvatica* L.) and oak (*Quercus petraea* (Matt.) Liebl.) obtained from thinning,  
663 and their relationship to structural parameters. *Annals of Forest Science* 78: 81.  
664 <https://doi.org/10.1007/s13595-021-01103-x>
- 665 R Core Team 2018. R: A language and environment for statistical computing. R Foundation for  
666 Statistical Computing, Vienna, Austria.
- 667 Raven PH, Evert RF, Eichhorn SE. 2007. *The biology of plants*. Brussels: De Boeck.
- 668 Ross, R. J. (2010). *Wood handbook: wood as an engineering material*. USDA Forest Service,  
669 Forest Products Laboratory, General Technical Report FPL-GTR-190, 2010: 509 p. 1 v., 190.
- 670 Savidge RA. 2003. Tree growth and wood quality. In: *Wood quality and its biological basis*,  
671 edited by JR. Barnett and G. Jeronimidis, Blackwell scientific, Oxford, UK (ISBN: 978-1-405-  
672 14781-1): 1-29
- 673 Thibaut B. 2019. Three-dimensional printing, muscles and skeleton: mechanical functions of  
674 living wood. *Journal of Experimental Botany*, Volume 70, Issue 14, 1 July 2019, Pages 3453–  
675 3466. <https://doi.org/10.1093/jxb/erz153>
- 676 Thibaut B, Gril J. 2021. Tree growth forces and wood properties. *Peer Community Journal*,  
677 Volume 1, article no. e46. <https://doi.org/10.24072/pcjournal.48>
- 678 Trenčiansky M, Lieskovský M, Merganič J, Šulek R (2017). Analysis and evaluation of  
679 the impact of stand age on the occurrence and metamorphosis of red heartwood. *iForest* 10:  
680 605-610. – doi: 10.3832/ifor2116-010 [online 2017-05-15]
- 681